



The assessment of metabolite alteration induced by –OH functionalized multi-walled carbon nanotubes in mice using NMR-based metabolomics

Yasamin Baghdadchi^{1†}, Maryam Khoshkam^{2†}, Mojtaba Fathi^{1,3*}, Ahmad Jalilvand¹, Koorosh Fooladsaz¹, Ali Ramazani^{3*}

¹Zanjan Metabolic Diseases Research Center, Zanjan University of Medical Sciences, Zanjan, Iran

²Chemistry Group, Faculty of Basic Sciences, University of Mohaghegh Ardabili, Ardabil, Iran

³Cancer Gene Therapy Research Center, Zanjan University of Medical Sciences, Zanjan, Iran

Article Info



Article Type:

Original Article

Article History:

Received: 15 June 2017

Revised: 27 Nov. 2017

Accepted: 29 Nov. 2017

ePublished: 6 Dec. 2017

Keywords:

Chemometrics,
 Metabolomics,
 Multi-walled carbon
 nanotubes,
 NMR,
 Toxicity

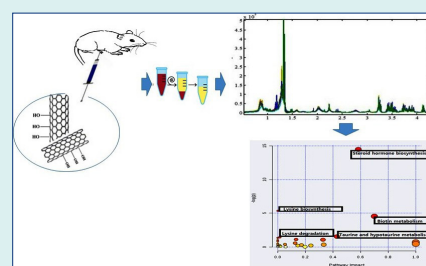
Abstract

Introduction: There is a fundamental need to characterize multiwalled carbon nanotubes (MWCNTs) toxicity to guarantee their safe application. Functionalized MWCNTs have recently attracted special interest in order to enhance biocompatibility. The aim of the current work was to study the underlying toxicity mechanism of the -OH-functionalized MWCNTs (MWCNTs-OH), using the powerful NMR-based metabolomics technique.

Methods: Following intraperitoneal single-injection of mice with 3 doses of MWCNTs-OH and one control, samples were collected at four time points during 22-days for NMR, biochemistry, and histopathology analysis. Metabolome profiling and pathway analysis were implemented by chemometrics tools and metabolome databases.

Results: Based on the ¹H-NMR data, metabolic perturbation induced by MWCNTs-OH were characterized by altered levels of steroid hormones, including elevated androgens, estrogens, corticosterone, and aldosterone. Moreover, increased L-lysine, amino adipate, taurine and taurocholic acid and decreased biotin were observed in the high-dose group (1 mg.kg⁻¹ B.W.) compared to the control. The findings also indicated that steroid hormone biosynthesis, lysine biosynthesis, and biotin metabolism are the most affected pathways by MWCNTs-OH.

Conclusion: These pathways can reflect perturbation of energy, amino acids, and fat metabolism, as well as oxidative stress. The data obtained by biochemistry, metabolomics, and histopathology were in good agreement, proving that MWCNTs-OH was excreted within 24 h, through the biliary pathway.



Introduction

Carbon nanotubes (CNTs) are a well-known member of the nanomaterial family.¹ They are cylindrical in shape, several millimeters in length and nanometers in diameter, and hence, a high length-to-diameter ratio.² These nanomaterials are one of the most promising engineered nanomaterials used in biomedical technologies.³ CNTs are categorized into 2 types of (i) single-walled carbon nanotubes (SWCNTs) and (ii) multi-walled carbon nanotubes (MWCNTs).⁴ In the realm of nanomedicine, MWCNTs have recently been used for different purposes, such as antitumor immunotherapy, infection therapy, and

as a delivery system for the neurodegenerative diseases.⁵⁻⁷ Nevertheless, there are significant challenges in terms of their toxicity and potential risk to human health.⁸ Composition, size, shape and surface chemistry are important factors to determine nanomaterial properties. Therefore, biodistribution and toxicity of nanomaterials must be investigated before they can be used safely in the clinic.^{9,10} Some deleterious effects occur due to the aggregation, nonpolar surface, and hydrophobicity of these nanomaterials.¹¹ Functionalization generally renders CNTs more solubility and biocompatibility. Thus, the functionalization can change the biological behavior

[†]These authors equally contributed to the study.

*Corresponding authors: Ali Ramazani, Email: ramazania@zums.ac.ir; Mojtaba Fathi, Email: m_fathi@zums.ac.ir



and toxicity of CNTs.¹² However, little is known about the altered toxicity of the functionalized MWCNTs.¹³

Most studies introduced oxidative stress, inflammation, and fibrosis as a potential mechanism of CNTs toxicity.^{14,15} *In vitro* data on MWCNTs-OH cytotoxicity indicated decreased viability, resultant from programmed cell death or apoptosis as well as indirect and oxidative DNA damage due to the direct contact of MWCNTs-OH with DNA even in low concentration (10 µg/mL) after 24 hours in human epithelial cells (A549). Also, lack of the lactate dehydrogenase (LDH) release revealed that MWCNTs-OH penetration to the cells was coupled with no membrane damage.¹⁶ Furthermore, 100 µg/mL of MWCNTs-OH led to cell cycle delay and a slight increase of apoptosis in MCF-7 and slowing down of the cell cycle in Caco-2 cell line but no effect on HL-60 and HFS cells after 72 hours. Particularly, in the cancer cell line of Caco-2, MWCNTs-OH not only was nontoxic but also inhibited cell proliferation.¹⁷ In addition, in A549 cells, MWCNTs-OH were localized in the cytoplasm and vacuoles and the internalization imposed no membrane damage or significant cytotoxicity. It did not even induce the release of inflammatory factors of IL-6, IL-8 and TNF-α.¹³ Yet, the toxic potential of MWCNTs-OH is rife with numerous gaps that need to be addressed. Although recent studies have revealed the cytotoxic, genotoxic and inflammatory effects of MWCNTs-OH, to date, the *in vivo* metabolic alterations arising from exposure to MWCNTs -OH remain unknown and need to be investigated by metabolomics approach.

Metabolites are the best markers to reveal the effects of toxins and drugs, and metabolomics studies provide valuable information by profiling the metabolic changes induced by nanomaterials. Moreover, sampling from one subject at different time intervals by metabolomics technologies provides a more dynamic measurement of toxicity.^{18,19} Taken together, metabolomics approaches have the potential to reveal biomarkers of nanoparticle exposure. Thus, this technology can be in favor of investigating the molecular mechanisms of nanoparticle-induced toxicity.^{20,21}

Proton NMR spectroscopy is a robust technique in metabolic profiling. It brings the opportunities of detecting thousands of metabolites in complex samples of various biofluids.^{18,22} The toxic effects of nanomaterials and xenobiotics are assessable through NMR-based metabolomics.²³

Following our research in nanotoxicology,^{24,25} the current work is an *in vivo* nanotoxicology study to evaluate alterations of metabolites as a result of -OH functionalized MWCNTs (MWCNTs-OH) exposure. Mice were dosed with 3 concentrations (0.25, 0.5 and 1 mg/kg B.W.) of MWCNTs-OH through intraperitoneal injection. These doses were selected based on the previous *in vivo* toxicology studies of CNTs in mice.²⁶⁻²⁸ The serum samples were collected at 4 time points. The ¹HNMR-spectroscopy coupled with pattern recognition analysis was applied

to the samples to characterize the perturbations due to MWCNTs-OH. In addition, clinical chemistry analysis and histopathological examination were performed to validate the results. This work may provide a novel insight into the underlying biological interactions of MWCNTs-OH in the living system.

Materials and Methods

Materials

The -OH functionalized MWCNTs with the purity of >95% synthesized by US Research Nanomaterial, Inc. (Houston, USA) were purchased from Nano Pasargad Novin Company (Tehran, Iran). According to the manufacturer, the outside diameter of CNTs is 10 to 20 nm; the inside diameter, 5 to 10 nm, and the length was 10 to 30 µm. Information on the purchased MWCNTs-OH is available at www.us-nano.com with the Stock#: US4307. Tween-80 was purchased from IRO Group Inc. (Tehran, Iran) and the D₂O was obtained from Pad-Kimia Novin Company, (Tehran, Iran). All the other chemicals used in the experiment were purchased from the Sigma-Aldrich (St. Louis, USA) and Merck (Kenilworth, USA).

Characterization techniques

Prior to performing experiments, the main properties of the purchased material were evaluated. Transmission electron microscopy (TEM) was used to determine the diameter and length of MWCNTs. Following deposition of MWCNTs-OH on TEM grid and allowing it to dry, the grid was set inside the TEM (PHILIPS CM30, Eindhoven, Netherlands) to observe the sample. Dynamic light scattering was performed at room temperature using a Nano Zetasizer (Malvern Instruments, Malvern, Workshoreshire, UK). The functional group was investigated via Fourier transform infrared spectroscopy (FT-IR) analysis (Thermo Fisher Scientific Inc., Waltham, USA).

Suspension preparation

First, 6 mg MWCNTs-OH was dispersed in 40 mL 0.9% normal saline containing 1% Tween-80. Then, the suspension was ultrasonicated for 60 min at 47°C. The resulted suspension was considered as stock suspension. With the injection of 0.2 mL volume from this suspension, a dose of 1 mg/kg MWCNTs-OH were obtained. To provide 0.5 mg/kg, 5 mL of stock suspension was added to 5 mL of the solvent (normal saline 0.9% containing 1% Tween-80) and 0.2 mL of this suspension was injected. Finally, 2.5 mL of the stock suspension was added to 7.5 mL of the solvent (normal saline 0.9% containing 1% Tween-80). By injecting 0.2 mL of this suspension, a dose of 0.25 mg/kg was obtained.

Treatment of animals and dosing

Eighty healthy adult male NMRI mice were purchased from animal laboratory center of Baqiyatallah University of Medical Sciences (Tehran, Iran), at the age of 6-8 weeks

and average body weight of 30 ± 2 g. The animals were randomly housed into 4 groups (20 mice per group) in metabolic cages (5 mice per cage). Mice were kept at the temperature of $22 \pm 2^\circ\text{C}$ and relative air humidity was 40%–60% and had 12 h: 12 h dark/light cycle. Mice were fed ad libitum and had free access to tap water. After 1 week of adaptation, the dosing process started. The control group received only solvent (a suspension of 0.9% saline and 1% Tween-80). The other 3 were classified as low-, medium-, and high-dose groups (L-dose, M-dose, and H-dose), and respectively received 0.25, 0.5, and 1 mg/kg B.W. of MWCNTs-OH. The administration was single-injection and performed intra-peritoneally to simulate therapeutic uses.

Preparation of serum samples

Blood samples were drawn from the hearts of 5 mice per group ($n = 5$) at 24 hours, 48 hours, 7 days, and 22 days post-injection under anesthesia. Next, the blood samples were set at room temperature for 30 min. Next, the samples were centrifuged at 5000 xg for 10 minutes at 4°C to obtain serum. The serum specimens were pooled together and were divided into 2 parts, including (i) one for NMR analysis, and (ii) one for the biochemical analysis. All the samples were stored at -80°C until the experiment conducted.

$^1\text{H-NMR}$ experiments

Three hundred fifty microliters of pooled serum samples taken from mice of each group were mixed with 150 μL of D_2O . TMS was used as internal reference for chemical shift calibration and $^1\text{H-NMR}$ spectra were gathered by means of Bruker Avance 400 NMR Spectrometer (Rheinstetten, Germany). The standard Carr-Purcell-Meiboom-Gill spin-echo pulse sequence [RD- 90° -(τ - 180° - τ) n-ACQ] was applied by means of the water suppression and a weak irradiating pulse on the water peak during the saturation delay.

The spectra were acquired by 100 scans into 32 k data points. The $^1\text{H-NMR}$ spectrum was collected with a relaxation delay of 2.0 seconds, and acquisition time of 3.27 seconds.²²

Pre-processing of $^1\text{H-NMR}$ spectra

MestReC NMR software (version 4.7.0.0) was used for phase and baseline correction of NMR spectra. NMR spectra of plasma samples were segmented into integral regions of 0.003 ppm, for each spectrum corresponding to regions 0–9 ppm. The spectral regions from 4.7 to 5 ppm were removed for water resonance elimination. The spectral data were mean centered to nullify the variation of mice serums and reach the integrated data. The data were imported into MATLAB (R2098a; Mathworks, Natick, MA) for the multivariate statistical analysis. A home-written program was applied for the multivariate analysis. The principal component analysis (PCA) was applied to the data in order to reduce the dimension of

data by the definition of new coordination system, which is called principal components (PCs). These variables were considered as the linear combination of the primary variables (i.e., the chemical shifts in this study).

Partial least-squares discriminant analysis (PLS-DA) was used to optimize the separation between samples. To control the over-fitting and also the validation of the PLS-DA models, a permutation test and jackknife cross-validation were applied, respectively. The results get by PLS-DA is shown in forms of score plot and loading plot. The former shows the relation between the samples and the later shows the chemical shifts which are responsible for the separation of groups in datasets.

The most important chemical shifts contributing to group separation were selected using Variable Importance in Projection (VIP), which is a powerful supervised classification method in metabolomics studies.^{29,30}

Identification of metabolites and pathways

After maximum class separation, metabolites identified based on chemical shifts of class separation by means of the Human Metabolome Databases (HMDB).³¹ HMDB (<http://www.hmdb.ca>) is a freely available electronic database containing detailed information about small molecule metabolites found in the human body. MetaboAnalyst (<http://www.metaboanalyst.ca>) is a web server designed to comprehensive metabolomic data analysis that we applied to identify pathways associated with the obtained metabolites.³² The most affected pathways were extracted based on the false discovery rate (FDR). The increase or decrease in the amount of each altered metabolites in the pathways was compared with the same metabolites in control group with a P value less than 0.05.

Biochemical analysis of serum

Activities of main serum enzymes such as alanine aminotransferase (ALT), aspartate aminotransferase (AST), alkaline phosphatase (ALP), lactate dehydrogenase (LDH), as well as levels of important parameters, such as glucose (Glc), triglyceride (TG), total cholesterol (Tc), creatinine (Cr), bilirubin (BIL), blood urea nitrogen (BUN), and albumin (ALB) were detected in the serum samples using Mindray-bs-800 automatic analyzer (Mindray, China).

Histopathological examinations

After mice were euthanized, their kidneys, lungs, and left lateral lobes of the liver were removed and immediately washed with phosphate-buffered saline (PBS) to remove the blood. Next, the organs were fixed in 10% formalin, sectioned at 4 μm , and stained with hematoxylin and eosin. They were then examined under a light microscope.

Statistical analysis

Statistical analysis of biochemical parameters was performed using SPSS software, version 19 (IBM SPSS

statistics 19.0. Inc., Armonk, NY, USA). Data were presented as mean \pm standard deviations. Since we pooled the blood-samples of each group, the reading process was repeated (3 times) to measure every factor. Therefore, the number of replicates (n value) was 3. Paired-samples *t*-test was measured for each sampling value. *P* values less than 0.05 were considered statistically significant.

Results

Characterization of MWCNTs-OH

According to the TEM image (Fig. 1A), MWCNTs-OH were cylindrical hollow tubes; and the diameter and length of MWCNTs-OH were consistent with the information obtained by the manufacturer. As shown in Fig. 1B, the peak in size distribution curve shows larger size for the nanotubes. The DLS measurements usually show larger diameter as compared to TEM. Because in TEM only the inorganic core is estimated, while in the DLS analysis, the solvent layer is also considered. Fig. 2 represents the FT-IR spectra of the MWCNTs-OH. The area around 3400 cm^{-1} confirms the existence of the O-H group on the surface of the MWCNTs.

Biochemistry and histopathology

As shown in Table 1, most of the parameters expressed significant alteration at 24 hours post-injection in the H-dose group. Compared to the control group; the BUN, ALB and ALT were diminished and Glc was increased ($P < 0.05$). Compared to the L-dose group, BUN, BIL, AST, TG, and TC were altered ($P < 0.05$). And compared to the M-dose group, TG was decreased ($P < 0.05$).

Also in other time points, some significant alterations were observed in the H-dose group. At 48 hours post-injection, BUN (compared to the control group) and TG (compared to the control and L-dose group) were increased; and TC (compared to the L-dose group) was decreased ($P < 0.05$). At 7 days post-injection, ALP (compared to the control group), Glc (compared to the L-dose group) and TG (compared to the control group) were altered ($P < 0.05$). In addition, at 22-days post injection, TG was diminished compared to the L-dose group ($P < 0.05$).

To sum it up, as MWCNTs-OH did not increase the serum BUN and Cr, it can be concluded that the renal function has not been changed after the treatment. The decreased levels of the BUN in the H-dose group in 24 hours and 48 hours could be due to the different amounts of protein received by animal's nutrition. The altered levels of ALB, ALT, AST, BIL as well as Glc could be representative of alteration in the hepatic and pancreatic functions in 24 hours post-injection. Also, it is notable that TG levels in the H-dose group showed significant alteration in all the time points.

No significant histological damage was observed in the MWCNTs-OH-treated mice as compared to the control mice. All liver, lung, and kidney tissues appeared normal (Fig. 3). Applied doses of MWCNTs-OH in this study did

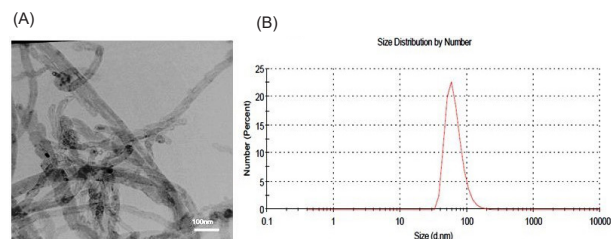


Fig. 1. (A) TEM image of MWCNTs-OH (B) Size distribution by number for MWCNTs-OH.

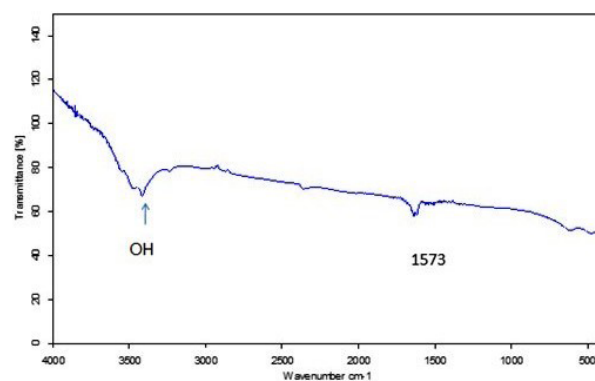


Fig. 2. FTIR spectra of MWCNTs-OH.

not induce any histological changes. Neither a mortality nor a weight loss induced by MWCNTs-OH was observed during the period of study.

¹H-NMR spectroscopic measurement of serum samples

The dose- and time-related toxicity induced by MWCNTs-OH was investigated using ¹H-NMR spectroscopic and pattern recognition analysis. Fig. S1 (Supplementary Data) shows the final binned NMR data of all samples (a) and bar and density plots of plasma samples before (b, d) and after mean centering (c, e). These plots illustrate the differences in data distributions before and after the normalization. Score plots of NMR spectra are depicted in Fig. S2 (Supplementary Data), indicating the group differences. The aim was to show the clustering of groups in 2-D space. Since we have pooled the blood samples of mice per group, each data point represents a pooled sample in a particular group. Samples were obtained from 4 groups (3 dosed and 1 control) in 4-time points (24 and 48 hours, 7 and 22 days). The sample 22 days in the control group was significantly different from other samples and detected as an outlier. Thus, this sample was removed from the control group, and there were totally 15 samples in 4 groups in the score plot. The distance between the points represents the differences between groups. As shown in the score plot after applying PLS-DA, the control group is separated greatly from dosed groups. The L-dose and H-dose groups were separated well from each other. However, the M-dose group had an overlap with both the L-dose and H-dose groups.

In Fig. S3 (Supplementary Data), a loading plot is

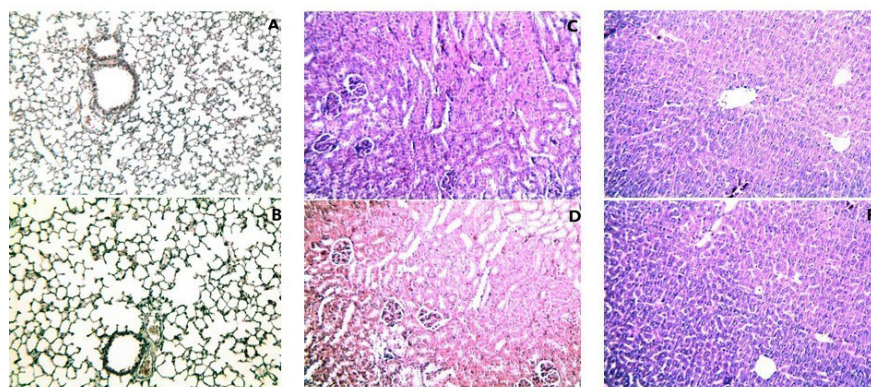


Fig. 3. Histopathological characterization of tissues. A) Lung from control group. B) Lung from the H-dose group. C) Kidney from the control group. D) Kidney from the H-dose group. E) Liver from the control group. F) Liver from the H-dose group. The images show H & E stained samples (magnification $\times 100$).

shown. Most of the points are piled near the origin point and only a few points are scattered (Fig. S3). The scattered points represent the chemical shifts responsible for the class separation. Thus, these scattered points would lead to the corresponding metabolites, which differ between groups.

Following the VIP score calculation, chemical shifts with a VIP score of higher than one were selected. The data bank of Human Metabolome Database (HMDB) was used to determine separated metabolites. The chemical shifts were selected based on the VIP scores, and uploaded to the HMDB site, to achieve the most probable metabolites contributing to discrimination.

The metabolites most likely altered by MWCNTs-OH are listed in Table 2. The prominent alterations related to the elevated levels of steroid hormones and intermediates of their biosynthesis. In fact, the discriminant metabolites are associated with metabolic pathways. To investigate these pathways, MetaboAnalyst³² (a metabolomics data analyzing database) was applied. The metabolic pathways most likely altered after exposure to the MWCNTs-OH are presented in Table 3 and Fig. 4. In these data, the hits illustrate how many metabolites from our uploaded data are matched with the metabolites of a specific pathway. There are different factors to evaluate the importance of the pathways, including raw *P* (the original *P* value

Table 1. Comparison of biochemical parameters between groups and time points

Group	TC	Cr	TG	BUN	ALT	AST	ALP	Glc	LDH	BIL	ALB
C24	112 \pm 2.0	0.5 \pm 0.05	180 \pm 4.0	29.2 \pm 0.2	75 \pm 3.0	154 \pm 5.0	469 \pm 17.0	154 \pm 4.0	1446 \pm 406	0.14 \pm 0.03	3.3 \pm 0.1
L24	104 \pm 2.0	0.46 \pm 0.04	132 \pm 2.0	26.5 \pm 0.5	71 \pm 6.0	211 \pm 7.0	365 \pm 5.0	163 \pm 6.0	2771 \pm 510	0.16 \pm 0.01	3.1 \pm 0.3
M24	103 \pm 4.0	0.4 \pm 0.02	251 \pm 5.0	25.6 \pm 0.2	48 \pm 11.0	196 \pm 6.0	240 \pm 4.0	141 \pm 1000	3228 \pm 425	0.13 \pm 0.02	3.1 \pm 0.1
H24	109 \pm 3.0 ^b	0.44 \pm 0.05	177 \pm 4.0 ^{b,c}	25 \pm 0.5 ^{a,b}	42 \pm 9.0 ^a	113 \pm 9.0 ^b	428 \pm 13.0	176 \pm 6.0 ^a	1844 \pm 514	0.1 \pm 0.01 ^b	2.9 \pm 0.05 ^a
C48	138 \pm 7.0	0.48 \pm 0.05	122 \pm 7.0	34.5 \pm 0.5	120 \pm 20	184 \pm 3.0	291 \pm 17.0	174 \pm 5.0	1915 \pm 471	0.2 \pm 0.04	3.4 \pm 0.4
L48	76 \pm 6.0	0.5 \pm 0.3	125 \pm 2.0	35.8 \pm 5.0	56 \pm 9.0	198 \pm 7.0	126 \pm 6.0	94 \pm 11.0	2752 \pm 462	0.10 \pm 0.03	3.4 \pm 0.3
M48	123 \pm 3.0	0.5 \pm 0.05	153 \pm 7.0	38.7 \pm 5.0	46 \pm 2.0	109 \pm 4.0	447 \pm 7.0	192 \pm 10.0	1627 \pm 505	0.10 \pm 0.02	3.4 \pm 0.7
H48	113 \pm 3.0 ^b	0.58 \pm 0.03	218 \pm 2.0 ^{a,b}	32.1 \pm 0.2 ^a	64 \pm 5.0	129 \pm 5.0	424 \pm 5.0	192 \pm 19.0	1124 \pm 480	0.12 \pm 0.03	3.0 \pm 0.5
C7	92 \pm 4.0	0.46 \pm 0.05	140 \pm 4.0	24 \pm 2.0	40 \pm 19.0	212 \pm 11.0	204 \pm 11.0	168 \pm 8.0	4306 \pm 456	0.06 \pm 0.05	2.6 \pm 0.1
L7	72 \pm 2.0	0.4 \pm 0.03	88 \pm 3.0	32.4 \pm 0.1	62 \pm 4.0	354 \pm 4.0	304 \pm 8.0	134 \pm 5.0	4874 \pm 522	0.08 \pm 0.02	2.6 \pm 0.4
M7	108 \pm 5.0	0.44 \pm 0.04	96 \pm 5.0	27.8 \pm 3.0	42 \pm 8.0	268 \pm 6.0	304 \pm 2.0	192 \pm 6.0	4584 \pm 424	0.07 \pm 0.03	3 \pm 0.2
H7	88 \pm 2.0	0.48 \pm 0.05	106 \pm 10.0 ^a	26 \pm 4.0	44 \pm 3.0	330 \pm 8.0	278 \pm 15.0 ^a	178 \pm 5.0 ^b	4560 \pm 490	0.1 \pm 0.03	3 \pm 0.5
C24	77 \pm 4.0	0.5 \pm 0.3	142 \pm 2.0	26.4 \pm 0.1	51 \pm 6.0	188 \pm 5.0	201 \pm 8.0	106 \pm 5.0	4290 \pm 466	0.13 \pm 0.04	2.7 \pm 0.3
L24	119 \pm 6.0	0.45 \pm 0.12	224 \pm 3.0	26 \pm 6.0	54 \pm 5.0	220 \pm 9.0	231 \pm 15.0	166 \pm 3.0	3267 \pm 524	0.12 \pm 0.02	2.8 \pm 0.9
M24	115 \pm 10.0	0.6 \pm 0.2	157 \pm 8.0	27.9 \pm 2.65	54 \pm 4.0	163 \pm 2.0	299 \pm 6.0	193 \pm 3.0	3163 \pm 490	0.13 \pm 0.03	3.1 \pm 0.3
H24	88 \pm 8.0	0.5 \pm 0.1	134 \pm 4.0 ^b	27.3 \pm 0.3	64 \pm 7.0	218 \pm 12.0	259 \pm 3.0	190 \pm 10.0	3200 \pm 511	0.16 \pm 0.02	3.3 \pm 0.4

TC: Total cholesterol (mg/dL). LDL: Low density lipoprotein (mg/dL). Cr: Creatinine (mg/dL). TG: Triglyceride (mg/dL). BUN: Blood urea nitrogen (mg/dL). ALT: Alanine aminotransferase (IU/L). AST: Aspartate aminotransferase (IU/L). ALP: Alkaline phosphatase (IU/L). Glc: Glucose (mg/dL). LDH: Lactate dehydrogenase (IU/L). BIL: Bilirubin (mg/dL). ALB: Albumin (g/dL). C24: Control group at 24 h. L24: L-dose group at 24 h. M24: M-dose group at 24 h. H24: H-dose group at 24 h. C48: Control group at 48 h. L48: L-dose group at 48 h. M48: M-dose group at 48 h. H48: H-dose group at 48 h. Moreover, the groups in each time-point were shown with the same color. Altered parameters were indicated by ^a (Compared to the control group, $P < 0.05$), ^b (Compared to the Low-dose group, $P < 0.05$) and ^c (Compared to the Medium-dose group, $P < 0.05$).

Table 2. The MWCNTs-OH induced variation in the endogenous metabolites compared to control group

Number	Metabolites	Query	Chemical shifts	L-dose	M-dose	H-dose
1	Cholesterol	HMDB00067	0.66(s), 1.17(m), 6.38(s), 6.62(s)	↓	↑	↑
2	Cholesterol sulfate	HMDB00653	0.82(s), 1.35(m), 1.45(m), 6.41(s), 6.62(s)	↑	↑	↑
3	Estradiol	HMDB00151	0.67(s), 3.71(s)	↓	↑	↑
4	Estriol	HMDB00153	0.83(s), 3.71(s)	↓	↑	↑
5	Estrone	HMDB00145	0.96(s), 0.95(m), 0.88(d), 0.63(s)	↓	↑	↑
6	2-Methoxyestradiol	HMDB00405	1.17(s), 1.21(s), 3.31(s), 5.62(s)	↑	↑	↑
7	2-Hydroxyestradiol	HMDB03962	1.761(m), 1.765(m), 1.777(m), 1.782(m), 2.234(t), 2.326(m), 2.335(m)	↑	↑	↑
8	16 α -Hydroxyestrone	HMDB00335	0.9(s), 1.05(s), 1.57(m)	↑	↑	↑
9	2-Hydroxyestrone	HMDB00343	0.92(s), 1.21(s)	↑	↑	↑
10	2-Methoxyestrone	HMDB00010	0.68(s), 0.81-0.85(m), 0.92-0.93(m)	↑	↑	↑
11	Ethiocolanolone	HMDB00490	0.68(s), 0.79(m), 0.85(dd), 0.96(m), 1.01(m), 1.55(s)	↑	↑	↑
12	Testosterone	HMDB00234	1.54(m), 1.01(s), 0.85(d)-0.92(d), 0.68(s)	↑	↑	↑
13	Androstendione	HMDB00053	1.54(m), 1.01(s), 0.85(d)-0.92(d), 0.68(s)	↓	↓	↑
14	Androstenedione	HMDB00899	0.65(s), 0.84-0.85(dd), 0.89-0.90(m), 0.95	↑	↑	↑
15	Dehydroepiandrosterone	HMDB00077	0.81(s), 1.38(s)	↑	↑	↑
16	17 α -Hydroxypregnenolone	HMDB00363	0.47(s), 1.32(m), 2.13(m), 5.64(s)	↓	↑	↑
17	17-Hydroxyprogesterone	HMDB00374	1.66(m), 1.03(s), 0.88(s)	↓	↑	↑
18	17 α ,20 α -Dihydroxypregn-4-en-3-on	HMDB11653	0.7(s), 1.19(s)	↑	↓	↑
19	Cortisone	HMDB02802	0.66(s), 3.51(s), 6.42-6.43(d), 7.03-7.04(m)	↑	↓	↑
20	Corticosterone	HMDB01547	0.66(s), 1.23(m), 2.68(m), 3.29(t), 6.42(d), 650(dd), 7.03(d)	↓	↑	↑
21	Progesterone	HMDB01830	0.86(s), 0.98(s)	↑	↑	↑
22	Deoxycorticosterone	HMDB00016	0.535(s), 0.797(s), 0.87(dd), 0.92(d), 1.37(s)	↑	↑	↑
23	Aldosterone	HMDB00037	5.74(s), 2.13(s), 1.2(s), 0.68(s)	↑	↑	↑
24	L-Lysine	HMDB00182	1.74-1.77(m), 1.9(m), 2.06-2.07(q), 2.37-2.40(t), 3.03-3.06(td), 3.58-3.60(t), 3.73-3.76(t)	↑	↑	↑
25	Saccharopine	HMDB00279	0.804(s), 1.206(s), 1.564(m)	↑	↓	↓
26	Aminoacidate	HMDB00510	0.66(s), 1.17(m), 6.38(s), 6.62(s)	↑	↓	↑
27	Biotin	HMDB00030	0.82(s), 1.35(m), 1.45(m), 6.41(s), 6.62(s)	↑	↓	↓
28	Biocytin	HMDB03134	0.67(s), 3.71(s)	↓	↓	↓
29	Taurine	HMDB00251	0.83(s), 3.71(s)	↑	↑	↑
30	Taurocholic acid	HMDB00036	0.96(s), 0.95(m), 0.88(d), 0.63(s)	↓	↑	↑
31	Pipecolic acid	HMDB00070	1.17(s), 1.21(s), 3.31(s), 5.62(s)	↑	↓	↓

Table 3. The altered metabolic pathways in serum samples due to MWCNTs-OH administration

Pathway name	Total	Hits	Raw p Value	FDR	Impact
Steroid hormone biosynthesis	72	23	5.1944E-7	4.2594E-5	0.58352
Lysine biosynthesis	4	3	0.0046416	0.19031	0.0
Biotin metabolism	5	3	0.01068	0.29191	0.7
Taurine and hypotaurine metabolism	8	2	0.21281	1.0	0.42857
Lysine degradation	23	4	0.23462	1.0	0.01471

Hits is the actually matched number from the user uploaded data, Raw p is the original p value calculated from the enrichment analysis, FDR p is the p value adjusted using False Discovery Rate, Impact is the pathway impact value calculated by pathway topology analysis.

calculated from the enrichment analysis), and the FDR (adjusted using False Discovery Rate). Furthermore, there was an impact calculated by the pathway topology to show the impact of pathways. To provide a better understanding of each pathway's importance, the pathway topology analysis is presented in Fig. 4, and it is available from MetaboAnalyst.

Discussion

Before starting the production of functionalized commercial MWCNTs for the biomedical application, it is essential to evaluate their toxicity in biological systems and at different concentrations.¹⁶ Metabolomics analysis is a suitable method for the *in vivo* screening of nanotoxicity, because of some advantages, including sensitivity,

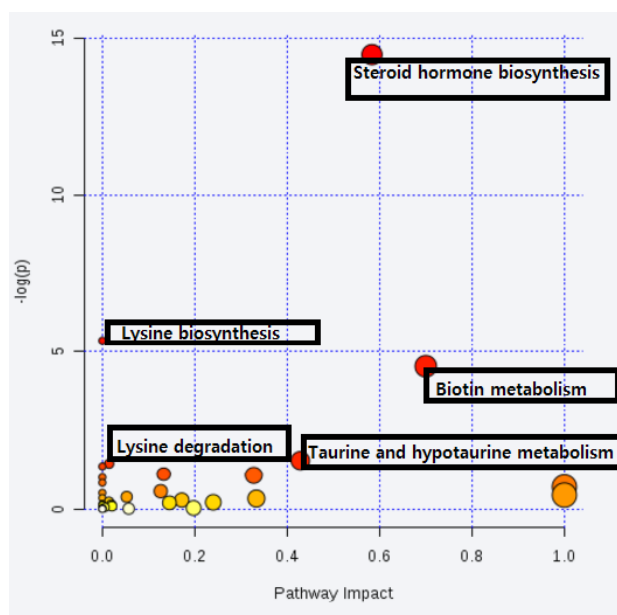


Fig. 4. Overview of the pathway analysis. The red circles are representative of the pathways with high importance. As the color grows brighter and shifts to orange, then yellow and white, the importance will diminish. Also, the higher a pathway is located, the more importance it poses.

timesaving, and high-throughput. This technique can provide valuable information on the biological behavior and the fate of nanomaterials by profiling the metabolic changes they induce.^{18,33}

Although the cell death or damage might not be reported following nanomaterial exposure, metabolite changes can still occur as a stress-response and cellular function.³⁴ Moreover, metabolites may change as a recovery response.^{19,35}

In the current work, ¹H-NMR-based metabonomics methods coupled with biochemistry and histopathology evaluations were applied to study the MWCNTs-OH-induced toxicity. Data showed that the most altered pathways following MWCNTs-OH administration are steroid hormone biosynthesis, lysine biosynthesis, biotin metabolism, taurine and hypotaurine metabolism, and lysine degradation. We discuss each pathway following the MWCNTs-OH toxicity mechanism.

Previous studies suggested that different types of nanoparticles can interact with the endocrine system. However, such notion seems like a critical evaluation because the endocrine interactions and toxicity of nanoparticles are poorly understood.³⁶ The steroid hormones have widespread physiological functions. They are involved in controlling metabolism, inflammation, immune function, salt and water balance, development of sexual characteristics, and tolerance of stress, injury, and illness.³⁷ Based on our data, 23 out of 70 metabolites of steroid hormone biosynthesis proved to be altered after being exposed to the MWCNTs-OH. Cholesterol level as a precursor of all steroid hormones was increased in the M-dose and H-dose groups compared to the control groups.

Also, dehydroepiandrosterone (DHEA), androstenedione, and androstenedione as precursors of testosterone and estrogens were changed. Androstenedione was increased in the H-dose group and decreased in the M-dose and L-dose. Cholesterol sulfate, DHEP, androstenedione, testosterone, and etiocholanolone (the main testosterone metabolite) were increased in all dosed-groups. One study provided evidence that the repeated administration of CNTs can induce stress-oxidative and reversible damage to the testis.³⁸ Another study suggested that one reason for the deleterious effects of nanomaterials on the male reproductive system is the alteration of biosynthetic and catabolic pathways of testosterone. As a result, they postulated that the alteration of normal levels of sex hormones, particularly testosterone, is an important issue in terms of making nanoparticles capable of disrupting the male reproductive system.³⁶ Carbon black nanoparticles, another carbon-based nanoparticle, induce expression of the steroidogenic acute regulatory protein (StAR) in the Leydig cells; this protein is an essential molecule in the biosynthesis of testosterone.³⁹ Our data are consistent with this study as the exposure to MWCNTs-OH was found to increase the biosynthesis of testosterone and its metabolites. In addition, estradiol, estrone, and estril as main forms of estrogenic steroids were increased in the M-dose and H-dose group. Further, the increased levels of their metabolites including 2-methoxyestradiol, 2-hydroxyestradiol, 16 α -hydroxyestrone, 2-methoxyestrone and 2-hydroxyestrone, were observed in all dosed-groups. There is a lack of information on the estrogenic effects of nanoparticles. However, it is assumed that estrogenic metabolites have changed, in large part due to the alteration of androgenic metabolites. Moreover, progesterone was increased. Progesterone is known as an important precursor for the synthesis of cortisol, estrogen, testosterone, and DHEA in the steroid hormone biosynthesis.⁴⁰ Since the mice tested in this study were male, it is postulated that progesterone has increased as a result of the increased levels of aforementioned hormones. Aldosterone and its precursor deoxycorticosterone have also been increased in all dosed-groups compared to the control. In addition, 17 α -hydroxypregnenolone, 17 α -hydroxyprogesterone, 17 α , 20 α -dihydroxypregn-4en-3on as intermediates of corticosterone pathway, along with corticosterone and cortisone, were increased in the H-dose group. A recent study indicated that the MWCNTs-OH, via oral administration, led to 44.3% weight gain in mice, which was postulated to be related to the alteration of steroid hormone levels observed previously.⁴¹ Having showed the increased levels of steroid hormones, our data could confirm this hypothesis.

Four metabolites are involved in the lysine biosynthesis pathway. Our data showed that MWCNTs-OH altered 3 of them. L-lysine was increased in all dosed-groups. Saccharopine was increased in the L-dose group and decreased in the M-dose and H-dose groups as

compared to the controls. Amino adipate decreased in the M-dose and increased in the L-dose and H-dose group. Amino adipate is a potential marker of oxidative stress⁴²; and oxidative stress as well as the production of reactive oxygen species (ROS) have been implicated in the toxicity of CNTs in several studies.^{27,28,43,44} Under the condition of stress-oxidative, proteins become carbonylated from lysine, histidine or cysteine residue, which finally can alter proteins, which is a key mechanism in terms of the ROS production.^{45,46} Then ROS can cause oxidation of proteins, DNA or peroxidation of lipids⁴⁵ which had been reported as CNT's damages. One recent metabolomics study on SWCNTs showed that the liver injury induced by SWCNTs is due to the occurrence of stress oxidative, and stress oxidative damage and lipid peroxidation occurred because of the SWCNTs exposure.⁴⁷ Consistent with this result, the aforementioned manifestation of the increased level of amino adipate in the H-dose group can be a clue to the stress oxidative condition.

L-lysine is another altered metabolite in this pathway. Since carnitine is the main derivative of L-lysine, thus L-lysine alteration can alter carnitine. Carnitine as a carrier is essential for β -oxidation and facilitates fatty acids transferring through the inner mitochondrial membrane.⁴⁸ Therefore, β -oxidation of fatty acids may have been affected as a result of the L-lysine alteration.

Biotin, L-lysine, and biocytin are altered metabolites in this pathway. Biocytin is a low molecular weight analog of biotin that occurs as an intermediate in the metabolism of biotin⁴⁹; and it was decreased in all the dosed-groups after being exposed to the MWCNTs-OH. Biotin was increased in the L-dose but decreased in the M-dose and H-dose groups. Biotin (vitamin B₇) has numerous roles in metabolic pathways; where it is required for the metabolism of fatty acids, glucose, and amino acids. This vitamin is essential for the conversion of food into energy.⁵⁰ Thus, any alteration of biotin concentration can alter the metabolism of energy. Similarly, biotin is a major cofactor of carboxylase enzymes in the metabolic processes, including acetyl-CoA carboxylase in fatty acids synthesis and pyruvate carboxylase in gluconeogenesis. Thus, decreased levels of biotin in the M-dose and H-dose groups may cause enzymatic disorders in aforementioned pathways. Acetyl-CoA carboxylase as a rate-limiting enzyme involves in regulation of fatty acid biosynthesis. There is a strong possibility that biotin insufficiency can reduce the fatty acid synthesis. Moreover, in gluconeogenesis, pyruvate carboxylase generates oxaloacetate from pyruvate. Biotin insufficiency can also hamper this stage. Oxaloacetate is a vital substrate of tricarboxylic acid cycle and any factor that decreases its production may induce energy metabolism disturbance. The recent metabolomics study on SWCNTs provided evidence of blocked fat metabolism. Consistent with our data, this study postulated alteration of fat and energy metabolism in response to CNTs.⁴⁷

Our data also showed that L-lysine, saccharopine,

pipecolic acid, and amino adipate are altered during the lysine degradation. Amino adipate is a hallmark of protein oxidation through stress oxidative.⁵¹ Elevated amino adipate in the H-dose group might be an indication of the lysine degradation through stress oxidative. Pipecolic acid is a cyclic amino acid occurring during lysine degradation as an intermediate,⁵² which was decreased in the M-dose and H-dose groups and increased in the L-dose group as compared to the control groups. MWCNTs-OH treatment increased taurine in all the dosed-groups and taurocholic acid in the M-dose and H-dose groups. These two metabolites are involved in the pathways of taurine and hypotaurine metabolism as well as biosynthesis of primary bile acids. Taurine is a sulfur-containing amino acid, which is not used for the protein synthesis. Taurine is involved in several metabolic activities. The most important role of taurine is its involvement in the bile acid conjugation in the liver.⁵³ Following phagocytosis by kupffer cells in the liver, nanoparticles will be metabolized and excreted by the biliary system.⁵⁴ Therefore, it is probable that, in our study, the hepatobiliary secretion of MWCNTs-OH might occur due to the secretion of bile acids. Consistent with our findings, a study represented that if CNTs become more soluble in bile by functionalization, implying that they can be excreted into feces through the biliary pathway.⁵⁵ Another study reported the biliary excretion via detecting Raman signals of CNTs in the feces and intestines of mice. Thus, it was suggested that the clearance of CNTs from the reticuloendothelial system could be related to the biliary excretion into feces, while functionalization with the hydrophilic groups make the excretion faster.⁵⁶ Based on the biochemical analysis, the drop of BIL levels within 24 hours post-injection can confirm these findings. BIL decreased in the plasma because taurine can increase the BIL excretion.⁵⁷

Altogether, the biochemistry analysis revealed that all the measured factors except Cr, LDH, and ALP, were altered in the H-dose group compared to the control or the L-dose group at 24 h post-injection.

Because of an enhanced solubility of MWCNTs in the bile (by adding -OH groups on the surface of nanotubes) and the absence of any histological damage or accumulation of nanoparticles in removed organs, there will be a possibility for the biliary clearance of MWCNTs-OH within 24 hours. A recent study revealed that if MWCNTs become functionalized by -OH group, they will induce no damage to the cell membranes.¹³ Also in the cytotoxicity and genotoxicity study of OH-MWCNTs in pulmonary cells, it was proven that OH-MWCNTs can reach the nucleus without damaging cell membrane.¹⁶ Our observations confirm this finding since the data obtained by the biochemistry analysis revealed that ALP or LDH (as the indicators) did not increase after the treatment. Similarly, based on the NMR findings, choline and phosphocholine (as the main membrane constituents) were not among the altered metabolites.

Research Highlights

What is current knowledge?

✓ The unique properties of multi-walled carbon nanotubes (MWCNT) allow for their potential use in various biomedical devices and therapies.

✓ The elucidation of toxicity determinants of MWCNT is still incomplete.

✓ The *in vivo* toxicity mechanism of MWCNTs-OH is investigated.

What is new here?

✓ The most affected pathways were the biosyntheses of steroid hormone and lysine, and the biotin metabolism.

✓ Toxicity mechanism of MWCNTs-OH relies on the perturbation of amino acid and fat metabolism as well as stress oxidative.

✓ -OH functionalization of MWCNTs facilitates excretion via the biliary pathway and avoids cell membrane damage.

Conclusion

The present investigation showed that the metabonomics method can provide a deeper understanding of nanomaterial bio-impact by metabolic profiling of biofluids in animal models. In brief, our findings showed that MWCNTs-OH induced metabolic perturbations by altered levels of steroid hormones including elevated androgens, estrogens, corticosterone, and aldosterone. Furthermore, in H-dose group (1 mg.kg⁻¹ B.W.) the level of L-lysine, amino adipate, taurine and taurocholic acid were increased and the amount of biotin was decreased in comparison to the control group. These altered metabolites indicated that the steroid hormone biosynthesis, lysine biosynthesis, and biotin metabolism are the most affected pathways which can reflect the perturbation of energy, amino acid, fatty acid metabolism, and oxidative stress. Moreover, our findings supported the recently reported results that -OH functionalization facilitates the biliary excretion and prevents the cell membrane damage. More profound investigation of these events and underlying toxicity mechanism could represent a precise molecular view of the *in vivo* behavior of MWCNTs-OH and therefore help in their safe application in biomedicine.

Ethical approval

This study was approved by Ethics committee for laboratory animals in Zanjan University of Medical Sciences (Zanjan, Iran). Ethics approval code is ZUMS.REC.1394.09.

Competing interests

The authors declare no conflict of interests.

Acknowledgment

We thank Ziba Akbari for helping in pathway analysis. This work financially was supported by Metabolic Disease Research Center of Zanjan University of Medical Sciences, Zanjan, Iran.

Supplementary Materials

Supplementary file 1 contains Figures S1-S3.

References

- Deng X, Jia G, Wang H, Sun H, Wang X, Yang S, et al. Translocation and fate of multi-walled carbon nanotubes *in vivo*. *Carbon* **2007**; 45: 1419-24. doi:10.1016/j.carbon.2007.03.035
- He H, Pham-Huy LA, Dramou P, Xiao D, Zuo P, Pham-Huy C. Carbon nanotubes: applications in pharmacy and medicine. *Biomed Res Int* **2013**; 2013. doi:10.1155/2013/578290
- Chortarea S, Clift MJ, Vanhecke D, Endes C, Wick P, Petri-Fink A, et al. Repeated exposure to carbon nanotube-based aerosols does not affect the functional properties of a 3D human epithelial airway model. *Nanotoxicology* **2015**; 9: 983-93. doi:10.3109/17435390.2014.993344
- Gulati N, Gupta H. Two faces of carbon nanotube: toxicities and pharmaceutical applications. *Crit Rev Ther Drug Carrier Syst* **2012**; 29:65-88. doi: 10.1615/CritRevTherDrugCarrierSyst.v29.i1.20
- Yang W, Thordarson P, Gooding JJ, Ringer SP, Braet F. Carbon nanotubes for biological and biomedical applications. *Nanotechnology* **2007**; 18: 412001. doi:10.1088/0957-4484/18/41/412001
- Jiang L, Liu T, He H, Pham-Huy LA, Li L, Pham-Huy C, et al. Adsorption behavior of pazufloxacin mesilate on amino-functionalized carbon nanotubes. *J Nanosci Nanotechnol* **2012**; 12: 7271-9. doi: 10.1166/jnn.2012.6562
- Digge M, Moon R, Gattani S. Applications of carbon nanotubes in drug delivery: a review. *Int J Pharmtech Res* **2012**; 4: 839-47. doi: 10.1016/j.cbpa.2005.10.005
- Mehra NK, Jain AK, Lodhi N, Raj R, Dubey V, Mishra D, et al. Challenges in the use of carbon nanotubes for biomedical applications. *Crit Rev Ther Drug Carrier Syst* **2008**; 25.
- Chen Y, Chen H, Shi J. *In vivo* bio-safety evaluations and diagnostic/therapeutic applications of chemically designed mesoporous silica nanoparticles. *Adv Mater* **2013**; 25: 3144-76. doi:10.1002/adma.201205292
- Mendez N, Liberman A, Corbeil J, Barback C, Viveros R, Wang J, et al. Assessment of *in vivo* systemic toxicity and biodistribution of iron-doped silica nanoshells. *Nanomedicine* **2017**; 13: 933-42. doi:10.1016/j.nano.2016.10.018
- Lee Y, Geckeler KE. Carbon nanotubes in the biological interphase: the relevance of noncovalence. *Adv Mater* **2010**; 22: 4076-83. doi: 10.1002/adma.201000746
- Mbeh D, França R, Merhi Y, Zhang X, Veres T, Sacher E, et al. *In vitro* biocompatibility assessment of functionalized magnetite nanoparticles: Biological and cytotoxicological effects. *J Biomed Mater Res A* **2012**; 100: 1637-46. doi: 10.1002/jbm.a.34096
- Ursini CL, Maiello R, Ciervo A, Fresegna AM, Buresti G, Superti F, et al. Evaluation of uptake, cytotoxicity and inflammatory effects in respiratory cells exposed to pristine and -OH and -COOH functionalized multi-wall carbon nanotubes. *J Appl Toxicol* **2015**. doi: 10.1002/jat.3228.
- Khalili Fard J, Jafari S, Eghbal MA. A review of molecular mechanisms involved in toxicity of nanoparticles. *Adv Pharm Bull* **2015**; 5:447-54. doi: 10.15171/apb.2015.061.
- Eom H-J, Jeong J-S, Choi J. Effect of aspect ratio on the uptake and toxicity of hydroxylated-multi walled carbon nanotubes in the nematode, *Caenorhabditis elegans*. *Environ Health Toxicol* **2015**; 30:e2015001. doi: 10.5620/eht.e2015001
- Ursini CL, Cavallo D, Fresegna AM, Ciervo A, Maiello R, Casciardi S, et al. Study of cytotoxic and genotoxic effects of hydroxyl-functionalized multiwalled carbon nanotubes on human pulmonary cells. *J Nanomater* **2012**; 2012: 7. doi:10.1155/2012/815979
- Bellucci S, Micciulla F, Bistarelli S, Dinicola S, Coluccia P, Cucina A, et al. Biological effects of functionalized multi-walled carbon nanotubes on human cancer and normal cell lines. *J Nanomed Nanotech* **2014**; 1: 1-5.
- Duarte IF. Following dynamic biological processes through NMR-based metabonomics: a new tool in nanomedicine? *J Control Release* **2011**; 153: 34-9. doi:10.1016/j.jconrel.2011.03.008
- Schnackenberg LK, Sun J, Beger RD. Metabolomics techniques in nanotoxicology studies. *Methods Mol Biol* **2012**; 926: 141-56. doi:10.1007/978-1-62703-002-1_10
- Ratnasekhar C, Sonane M, Satish A, Mudiam MKR. Metabolomics

- reveals the perturbations in the metabolome of *Caenorhabditis elegans* exposed to titanium dioxide nanoparticles. *Nanotoxicology* **2015**; 9: 994-1004. doi:10.3109/17435390
21. Lee S-H, Wang T-Y, Hong J-H, Cheng T-J, Lin C-Y. NMR-based metabolomics to determine acute inhalation effects of nano- and fine-sized ZnO particles in the rat lung. *Nanotoxicology* **2016**; 1-11. doi: 10.3109/17435390.2016.1144825
 22. Arjmand M, Akbari Z, Taghizadeh N, Shahbazzadeh D, Zamani Z. NMR-based metabolomics survey in rats envenomed by *Hemiscorpius lepturus* venom. *Toxicon* **2015**; 94: 16-22. doi: 10.1016/j.toxicon.2014.12.003
 23. Bu Q, Yan G, Deng P, Peng F, Lin H, Xu Y, et al. NMR-based metabolomic study of the sub-acute toxicity of titanium dioxide nanoparticles in rats after oral administration. *Nanotechnology* **2010**; 21: 125105. doi: 10.1088/0957-4484/21/12/125105
 24. Rajabi S, Ramazani A, Hamidi M, Naji T. *Artemia salina* as a model organism in toxicity assessment of nanoparticles. *Daru* **2015**; 23: 20. doi: 10.1186/s40199-015-0105-x
 25. Habibzadeh M, Rostamizadeh K, Dalali N, Ramazani A. Preparation and characterization of PEGylated multiwall carbon nanotubes as covalently conjugated and non-covalent drug carrier: A comparative study. *Mater Sci Eng C* **2017**; 74: 1-9. doi:10.1016/j.msec.2016.12.023
 26. Carrero-Sanchez JC, Elias AL, Mancilla R, Arrellin G, Terrones H, Laclette JP, et al. Biocompatibility and toxicological studies of carbon nanotubes doped with nitrogen. *Nano Lett* **2006**; 6: 1609-16. doi: 10.1021/nl060548p
 27. Patlolla A, McGinnis B, Tchounwou P. Biochemical and histopathological evaluation of functionalized single-walled carbon nanotubes in Swiss-Webster mice. *J Appl Toxicol* **2011**; 31: 75-83. doi: 10.1002/jat.1579
 28. Shvedova AA, Kisin E, Murray AR, Johnson VJ, Gorelik O, Arepalli S, et al. Inhalation vs. aspiration of single-walled carbon nanotubes in C57BL/6 mice: inflammation, fibrosis, oxidative stress, and mutagenesis. *Am J Physiol Lung Cell Mol Physiol* **2008**; 295: L552-65. doi: 10.1152/ajplung.90287.2008
 29. Brereton RG, Lloyd GR. Partial least squares discriminant analysis: taking the magic away. *J Chemom* **2014**; 28: 213-25. doi: 10.1002/cem.2609
 30. Westerhuis JA, Hoefsloot H, Smit S, Vis DJ, Smilde AK, van Velzen EJJ, et al. Assessment of PLS-DA cross validation. *Metabolomics* **2008**; 4: 81-9. doi: 10.1007/s11306-007-0099-6
 31. Wishart DS, Tzur D, Knox C, Eisner R, Guo AC, Young N, et al. HMDB: the Human Metabolome Database. *Nucleic Acids Res* **2007**; 35: D521-6. doi: 10.1093/nar/gkl923
 32. Xia J, Mandal R, Sinelnikov IV, Broadhurst D, Wishart DS. MetaboAnalyst 2.0—a comprehensive server for metabolomic data analysis. *Nucleic Acids Res* **2012**; 40: W127-W33. doi: 10.1093/nar/gks374
 33. Lei R, Wu C, Yang B, Ma H, Shi C, Wang Q, et al. Integrated metabolomic analysis of the nano-sized copper particle-induced hepatotoxicity and nephrotoxicity in rats: A rapid in vivo screening method for nanotoxicity. *Toxicol Appl Pharmacol* **2008**; 232: 292-301. doi: 10.1016/j.taap.2008.06.026
 34. Feng J, Li J, Wu H, Chen Z. Metabolic responses of HeLa cells to silica nanoparticles by NMR-based metabolomic analyses. *Metabolomics* **2013**; 9: 874-86. doi: 10.1007/s11306-013-0499-8
 35. Zhang B, Zhang H, Du C, Ng QX, Hu C, He Y, et al. Metabolic responses of the growing *Daphnia similis* to chronic AgNPs exposure as revealed by GC-Q-TOF/MS and LC-Q-TOF/MS. *Water Res* **2017**; 114: 135-43. doi: 10.1016/j.watres.2017.02.046
 36. Iavicoli I, Fontana L, Leso V, Bergamaschi A. The effects of nanomaterials as endocrine disruptors. *Int J Mol Sci* **2013**; 14: 16732-801. doi: 10.3390/ijms140816732
 37. Yadav R, Yadav N, Kharya MD. Steroid Chemistry and Steroid Hormone Action: A Review. *Asian J Res Chem* **2014**; 7: 964-9.
 38. Lu X, Liu Y, Kong X, Lobie PE, Chen C, Zhu T. Nanotoxicity: a growing need for study in the endocrine system. *Small* **2013**; 9: 1654-71. doi: 10.1002/sml.201201517
 39. West LA, Horvat RD, Roess DA, Barisas BG, Juengel JL, Niswender GD. Steroidogenic acute regulatory protein and peripheral-type benzodiazepine receptor associate at the mitochondrial membrane. *Endocrinol* **2001**; 142: 502-5. doi: 10.1210/endo.142.1.8052
 40. Jung-Testas I, Hu ZY, Baulieu EE, Robel P. Neurosteroids: biosynthesis of pregnenolone and progesterone in primary cultures of rat glial cells. *Endocrinology* **1989**; 125: 2083-91. doi: 10.1210/endo-125-4-2083
 41. Vasyukova IA, Gusev AA, Ubogov AY, Godymchuk AY. Study of MWNTS Influence upon Liver Histological and Histochemical Parameters in Laboratory Mice: Preliminary Results. *Adv Mat Res* **2015**; 1085: 376-83. doi: 10.4028/www.scientific.net/AMR.1085.376
 42. Zeitoun-Ghandour S, Leszczyszyn OI, Blindauer CA, Geier FM, Bundy JG, Stürzenbaum SR. *C. elegans* metallothioneins: response to and defence against ROS toxicity. *Mol Biosyst* **2011**; 7: 2397-406. doi: 10.1039/c1mb05114h
 43. Inoue K, Yanagisawa R, Koike E, Nishikawa M, Takano H. Repeated pulmonary exposure to single-walled carbon nanotubes exacerbates allergic inflammation of the airway: Possible role of oxidative stress. *Free Radic Biol Med* **2010**; 48: 924-34. doi: 10.1016/j.freeradbiomed.2010.01.013
 44. Muller J, Decordier I, Hoet PH, Lombaert N, Thomassen L, Huaux F, et al. Clastogenic and aneugenic effects of multi-wall carbon nanotubes in epithelial cells. *Carcinogenesis* **2008**; 29: 427-33. doi: 10.1093/carcin/bgm243
 45. Grimsrud PA, Xie H, Griffin TJ, Bernlohr DA. Oxidative stress and covalent modification of protein with bioactive aldehydes. *J Biol Chem* **2008**; 283: 21837-41. doi: 10.1074/jbc.R700019200
 46. Frohnert BI, Bernlohr DA. Protein carbonylation, mitochondrial dysfunction, and insulin resistance. *Adv Nutr* **2013**; 4: 157-63. doi: 10.3945/an.112.003319
 47. Lin B, Zhang H, Lin Z, Fang Y, Tian L, Yang H, et al. Studies of single-walled carbon nanotubes-induced hepatotoxicity by NMR-based metabolomics of rat blood plasma and liver extracts. *Nanoscale Res Lett* **2013**; 8: 1-11. doi: 10.1186/1556-276X-8-236
 48. Sharma S, Black SM. Carnitine homeostasis, mitochondrial function and cardiovascular disease. *Drug Discov Today Dis Mech* **2009**; 6: e31-e9. doi: 10.1016/j.ddmec.2009.02.001
 49. King MA, Louis PM, Hunter BE, Walker DW. Biocytin: a versatile anterograde neuroanatomical tract-tracing alternative. *Brain Res* **1989**; 497: 361-7. doi: 10.1016/0006-8993(89)90281-3
 50. Zempleni J, Hassan YI, Wijeratne SS. Biotin and biotinidase deficiency. *Expert Rev Endocrinol Metab* **2008**; 3: 715-24. doi: 10.1586/17446651.3.6.715
 51. Yuan W, Zhang S, Li S, Edwards JL. Amine metabolomics of hyperglycemic endothelial cells using capillary LC-MS with isobaric tagging. *J Proteome Res* **2011**; 10: 5242-50. doi: 10.1021/pr200815c
 52. Mihalik SJ, Moser HW, Watkins PA, Danks DM, Poulos A, Rhead WJ. Peroxisomal L-pipecolic acid oxidation is deficient in liver from Zellweger syndrome patients. *Pediatr Res* **1989**; 25: 548-52. doi: 10.1203/00006450
 53. Birdsall TC. Therapeutic applications of taurine. *Altern Med Rev* **1998**; 3: 128-36.
 54. Mendez N, Liberman A, Corbeil J, Barback C, Viveros R, Wang J, et al. Assessment of in vivo Systemic Toxicity and Biodistribution of Iron-doped Silica Nanoshells. *Nanomedicine* **2017**; 13:933-42. doi: 10.1016/j.nano.2016.10.018.
 55. Liu Z, Tabakman S, Welsch K, Dai H. Carbon nanotubes in biology and medicine: in vitro and in vivo detection, imaging and drug delivery. *Nano Res* **2009**; 2: 85-120. doi: 10.1007/s12274-009-9009-8
 56. Liu Z, Davis C, Cai W, He L, Chen X, Dai H. Circulation and long-term fate of functionalized, biocompatible single-walled carbon nanotubes in mice probed by Raman spectroscopy. *Proc Natl Acad Sci U S A* **2008**; 105: 1410-5. doi: 10.1073/pnas.0707654105
 57. Islambulchilar M, Asvadi I, Sanaat Z, Esfahani A, Sattari M. Effect of taurine on attenuating chemotherapy-induced adverse effects in acute lymphoblastic leukemia. *J Cancer Res Ther* **2015**; 11: 426. doi: 10.4103/0973-1482.151933